

AD-A051 187

ROME AIR DEVELOPMENT CENTER GRIFFISS AFB N Y
ANALYSIS OF THE MICROSTRIP DISK ANTENNA ELEMENT, (U)
NOV 77 A DERNERYD

F/G 9/5

UNCLASSIFIED

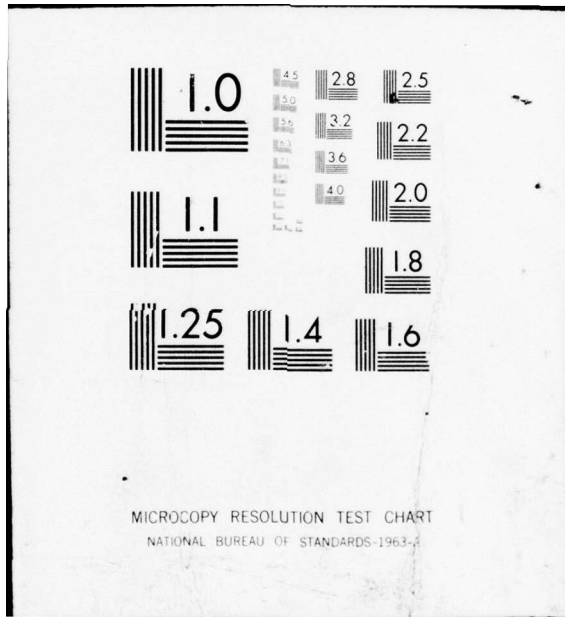
RADC-TR-77-383

NL

| OR |
AD
A051187



END
DATE
FILMED
4-78
DDC



AD A 051187

RADC-TR-77-383
IN-HOUSE REPORT
NOVEMBER 1977



2

Analysis of the Microstrip Disk Antenna Element

ANDERS DERNERYD

AD No. ~~1187~~
DDC FILE COPY

DDC
RECEIVED
MAR 14 1978
B

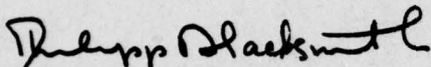
Approved for public release; distribution unlimited.

ROME AIR DEVELOPMENT CENTER
AIR FORCE SYSTEMS COMMAND
GRIFFISS AIR FORCE BASE, NEW YORK 13441

This report has been reviewed by the RADC Information Office (OI) and is releasable to the National Technical Service (NTIS). At NTIS it will be releasable to the general public, including foreign nations.

This technical report has been reviewed and approved for publication.

APPROVED:

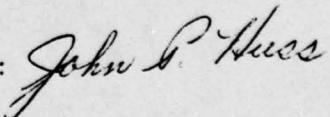


PHILIPP BLACKSMITH
Chief, Electromagnetic Systems Concepts Branch

APPROVED:



ALLAN C. SCHELL
Acting Chief
Electromagnetic Sciences Division

FOR THE COMMANDER: 

Plans Office

Unclassified
SECURITY CLASSIFICATION OF THIS PAGE (When Data Entered)

REPORT DOCUMENTATION PAGE		READ INSTRUCTIONS BEFORE COMPLETING FORM	
14	1. REPORT NUMBER RADC-TR-77-383	2. GOVT ACCESSION NO.	3. RECIPIENT'S CATALOG NUMBER
6	4. TITLE (and Subtitle) ANALYSIS OF THE MICROSTRIP DISK ANTENNA ELEMENT	5. TYPE OF REPORT & PERIOD COVERED In-House	6. PERFORMING ORG. REPORT NUMBER
10	7. AUTHOR(s) Anders/Derneryd	8. CONTRACT OR GRANT NUMBER(s)	
	9. PERFORMING ORGANIZATION NAME AND ADDRESS Deputy for Electronic Technology (RADC/EEA) Rome Air Development Center Hanscom AFB, MA 01731	10. PROGRAM ELEMENT, PROJECT, TASK AREA & WORK UNIT NUMBERS 62702F 46001402	11. REPORT DATE Nov 1977
	11. CONTROLLING OFFICE NAME AND ADDRESS Deputy for Electronic Technology (RADC/EEA) Rome Air Development Center Hanscom AFB, MA 01731	12. NUMBER OF PAGES 24	13. SECURITY CLASS. (of this report) Unclassified
	14. MONITORING AGENCY NAME & ADDRESS (if different from Controlling Office)	15a. DECLASSIFICATION/DOWNGRADING SCHEDULE	
16. DISTRIBUTION STATEMENT (of this Report) Approved for public release; distribution unlimited.			
17. DISTRIBUTION STATEMENT (of the abstract entered in Block 20, if different from Report)			
18. SUPPLEMENTARY NOTES This work was performed in a Post-Doctoral Program under the Southeastern Center for Electrical Engineering Education, Inc.			
19. KEY WORDS (Continue on reverse side if necessary and identify by block number) Antenna Microwave Microstrip			
20. ABSTRACT (Continue on reverse side if necessary and identify by block number) The circular microstrip antenna element is formed by a radiating disk closely spaced above a groundplane. It is modeled as a cylindrical cavity with magnetic walls that can be resonant in the TM modes. The far-fields and the radiation conductances for different mode structures have been cal- culated assuming a magnetic line current flowing around the perimeter of the disk. The directivity of the disk antenna excited in the dominant mode is between 4.8 dB and 9.9 dB, depending on the size.			

DDC
RECEIVED
MAR 14 1978
B

DD FORM 1 JAN 73 1473 EDITION OF 1 NOV 65 IS OBSOLETE

Unclassified
SECURITY CLASSIFICATION OF THIS PAGE (When Data Entered)

1

309 050

Yue

Unclassified

SECURITY CLASSIFICATION OF THIS PAGE(When Data Entered)

20. Abstract (Continued)

Losses, due to imperfect supporting dielectric and due to finite conductivity of the conductors, have been derived by means of a perturbation technique assuming small losses don't drastically change the fields from their loss-free case. Graphs are given for design purposes showing the input impedance, the Q-factor, and the radiation efficiency at resonance for different modes and spacings. The air-filled microstrip antenna has the highest efficiency and the broadest bandwidth for a given frequency.

Unclassified

SECURITY CLASSIFICATION OF THIS PAGE(When Data Entered)

Contents

1. INTRODUCTION	5
2. RADIATION PATTERN	6
3. RESONANCE FREQUENCIES	8
4. RADIATED POWER	10
5. DIRECTIVITY	11
6. DIELECTRIC LOSSES	12
7. OHMIC LOSSES	13
8. INPUT IMPEDANCE	14
9. EFFICIENCY	17
10. QUALITY FACTOR	19
11. CIRCULAR POLARIZATION	22
12. SUMMARY AND DISCUSSION	23
REFERENCES	24

ACCESSION for	
NTIS	White Section <input checked="" type="checkbox"/>
DDC	Buff Section <input type="checkbox"/>
UNANNOUNCED	<input type="checkbox"/>
JUSTIFICATION	_____
BY _____	
DISTRIBUTION/AVAILABILITY CODES	
Dist.	AVAIL. and/or SPECIAL
A	

Illustrations

1. Circular Microstrip Disk Antenna Element	7
2. Correction of Disk Radius Due to Stray Fields	9
3. Radiation Conductance at Resonance of a Disk Antenna Excited in the TM Modes	11
4. Directivity at Resonance of a Disk Antenna Excited in the TM_{1m} Modes	12
5. Equivalent Dielectric Conductance at Resonance of a Disk Antenna Excited in the TM_{n1} Modes	13
6. Equivalent Ohmic Conductance at Resonance of a Disk Antenna Excited in the TM_{n1} Modes	15
7. Normalized Input Impedance at Resonance of a Disk Antenna Excited in the TM_{n1} Modes as a Function of the Feed Point	15
8. Total Input Conductance at Resonance of a Disk Antenna Excited in the TM_{11} Mode	16
9. Total Input Conductance at Resonance of a Disk Antenna Excited in the TM_{21} Mode	16
10. Radiation Efficiency at Resonance of a Disk Antenna Excited in the TM_{11} Mode	17
11. Radiation Efficiency at Resonance of an Air-Filled Disk Antenna Excited in the TM_{11} Mode	18
12. Radiation Efficiency at Resonance of a Disk Antenna Excited in the TM_{21} Mode	18
13. Radiation Efficiency at Resonance of an Air-Filled Disk Antenna Excited in the TM_{21} Mode	19
14. Quality Factor at Resonance of a Disk Antenna Excited in the TM_{11} Mode	21
15. Quality Factor at Resonance of an Air-Filled Disk Antenna Excited in the TM_{11} Mode	21
16. Axial Ratio of a Circularly Polarized Disk Antenna Excited in the TM_{11} Mode	22

Analysis of the Microstrip Disk Antenna Element

I. INTRODUCTION

The designer of microstrip circuits is often faced with the questions of what the best substrate thickness is and what dielectric constant should be used, as low loss is desirable. The particular circuit may be a resonator, which is a useful component in filters and circulators. The losses divide into ohmic, dielectric, and radiation losses. Since the radiation properties can be utilized, the use of a microstrip resonator as a radiating structure has become a very active field of research and development during the last few years. In contrast to non-radiating components, a high radiation efficiency and a low Q-factor are of prime importance for antenna elements.

The circular disk resonator has been used as a linearly or circularly polarized radiating structure¹ and as an element in arrays,^{2,3} but so far very few theoretical papers have been published. Two general analytical approaches have been

(Received for publication 11 November 1977)

1. Howell, J.Q. (1975) Microstrip antennas, IEEE Trans. Antennas Propagation, AP-23:90-93.
2. Parks, F.G., and Bailey, M.C. (1977) A low sidelobe microstrip array, IEEE AP-S Intl. Symp. Digest, pp. 77-80, June.
3. Stockton, R.J., and Hockensmith, R.P. (1977) Application of spherical arrays - a simple approach, IEEE AP-S Intl. Symp. Digest, pp. 202-205, June.

proposed to analyze microstrip radiating structures. One method⁴ models the microstrip element as a grid of wire segments and applies Richmond's reaction technique. The other approach⁵ uses the unimoment-Monte Carlo method to obtain the far field radiation patterns. The circular disk radiator excited in the dominant mode only has been modeled as a magnetic line current and analyzed theoretically.^{6, 7}

In this paper an extension of the work reported by Long et al⁷ is given. The circular disk microstrip antenna element is modeled as a cavity with a magnetic wall along the edge. The resonator excited in a general mode is analyzed theoretically both from a radiation and a network point of view. The purpose is to present graphs and relationships between the geometry of the disk and the radiation efficiency, and also to analyze the effect losses have on the overall Q-factor of the microstrip resonator.

2. RADIATION PATTERN

The microstrip radiating element consists of a radiating structure spaced a small fraction of a wavelength above a groundplane, allowing radiation only into the upper half space. A circular disk element supported by a dielectric sheet is shown in Figure 1. The disk is excited by a microstrip transmission line connected to the edge, or by a coaxial line from the back at the plan $\psi = 0$. The fields between the disk and the groundplane are similar to those obtained by considering the antenna to be a narrow cavity with a magnetic wall around the perimeter. Among the various modes that may be excited in such disk resonators are the TM_{nm} modes with respect to the z-axis. That structure has been analyzed⁸ and the fields inside the cavity are

-
4. Agrawal, P.K., and Bailey, M.C. (1976) An analysis technique for microstrip antennas, IEEE AP-S Intl. Symp. Digest, pp. 395-398, Oct.
 5. Coffey, E.L. (1977) Microstrip antenna far-field radiation pattern analysis using the unimoment-Monte Carlo method, IEEE AP-S Intl. Symp. Digest, pp. 276-279, June.
 6. Long, S.A., and Shen, L.C. (1977) The circular disc, printed circuit antenna, IEEE AP-S Intl. Symp. Digest, pp. 100-103, June.
 7. Long, S.A., et al (1977) The Theory of the Circular Disc, Printed Circuit Antenna, Technical Report TR-77-01, Electromagnetics Laboratory, Dept. of Electrical Engineering, Univ. of Houston, Houston, TX.
 8. Watkins, J. (1969) Circular resonant structures in microstrip, Electron. Lett. 5:524-525, Oct.

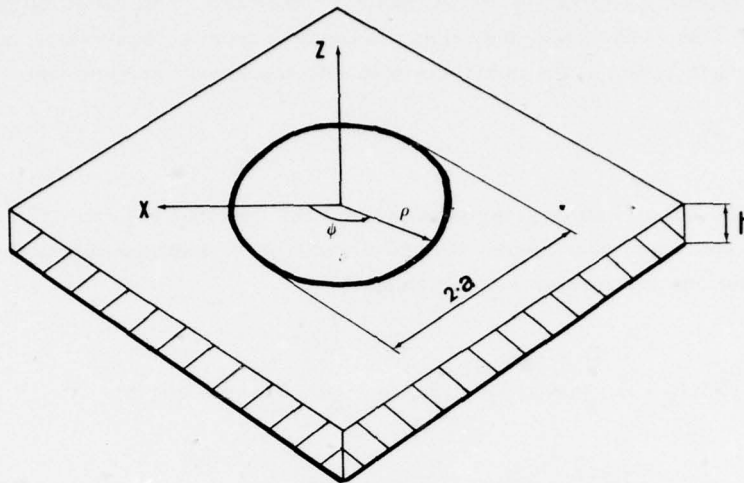


Figure 1. Circular Microstrip Disk Antenna Element

$$\begin{cases} E_z = E_0 \cdot J_n(k \cdot \rho) \cdot \cos n\psi \\ H_\rho = -\frac{j\omega \epsilon n}{k^2 \cdot \rho} \cdot E_0 \cdot J_n(k \cdot \rho) \cdot \sin n\psi \\ H_\psi = -\frac{j\omega \epsilon}{k} \cdot E_0 \cdot J'_n(k \cdot \rho) \cdot \cos n\psi \end{cases} \quad (1)$$

where k is the propagation constant in the dielectric, J_n is the Bessel function of the first kind and order n , and the prime indicates differentiation with respect to the argument.

Once the E-field inside the cavity is calculated, the K-current flowing on the disk can immediately be found as $K_\rho = H_\psi$ and $K_\psi = -H_\rho$. The open circuited edge condition requires that $J'_n(ka) = 0$, where a is the radius of the disk. Thus for each mode structure a particular radius can be found associated with the zeros of the derivative of the Bessel functions.

The radiation from the disk derives from the E-field across the aperture between the disk and the groundplane at $\rho = a$. Resistive-backed cholesteric liquid-crystal sheets were used⁹ to visualize the amplitude of the different mode patterns. The exact behavior of E_0 across the gap is not known, but for small

9. Kernweis, N.P., and McIlvanna, J.F. (1977) Liquid crystal diagnostic techniques an antenna design aid, Microwave Journal 20:47-51, 58, Oct.

spacings a realistic approximation is that it is constant. The radiation pattern of the circular disk in the upper half space is derived from an equivalent magnetic surface current acting at the aperture, and with the structure removed:

$$\bar{M} = 2\bar{E} \times \bar{n} \quad , \quad (2)$$

where \bar{n} is the normal unit vector pointing into the external region. The far fields in standard spherical coordinates may be found from a potential function or from the dual solutions of circular loop antennas:¹⁰

$$\begin{cases} E_{\theta} = -j^n \cdot k_0 \cdot \frac{e^{-jk_0 r}}{r} \cdot \frac{V_0 a}{2} \cdot B_M(k_0 \cdot a \cdot \sin \theta) \cdot \cos n\phi \\ E_{\phi} = j^n \cdot k_0 \cdot \frac{e^{-jk_0 r}}{r} \cdot \frac{V_0 a}{2} \cdot B_P(k_0 \cdot a \cdot \sin \theta) \cdot \cos \theta \cdot \sin n\phi \quad , \end{cases} \quad (3)$$

where

$$B_P(X) = J_{n-1}(X) + J_{n+1}(X)$$

$$B_M(X) = J_{n-1}(X) - J_{n+1}(X) \quad .$$

The edge voltage at $\psi = 0$ is defined as $V_0 = h \cdot E_0 \cdot J_n(ka)$. The far fields of the $n = 0$ mode are circular symmetric. The $n = 1$ mode is used in most applications because it is the only mode that doesn't have a zero in the radiation pattern normal to the structure.

3. RESONANCE FREQUENCIES

The resonance frequencies of the TM modes in the circular disk are given⁸ as

$$f_{nm} = \frac{\alpha_{nm} \cdot c}{2 \cdot \pi \cdot a_{\text{eff}} \cdot \sqrt{\epsilon_r}} \quad , \quad (4)$$

10. Martin, E.J. (1960) Radiation fields of circular loop antennas by a direct integration process, IRE Trans. Antennas Propagation AP-8:105-107, Jan.

where α_{nm} is the m -th zero of the derivative of the Bessel function of order n , c is the velocity of light in free space, and ϵ_r is the relative dielectric constant of the substrate. The dominant mode is the TM_{11} mode which has the lowest resonance frequency. An effective radius a_{eff} slightly larger than the physical one is defined,¹¹ taking into account the stray field along the edge of the resonator:

$$a_{\text{eff}} = a \cdot \left[1 + \frac{2 \cdot h}{\pi \cdot a \cdot \epsilon_r} \left(\ln \frac{\pi \cdot a}{2 \cdot h} + 1.7726 \right) \right]^{1/2} \quad a/h \gg 1 \quad (5)$$

This correction predicts the radius with less than a 2.5 percent error. The relation between the effective and the physical radius for different dielectric constants is shown in Figure 2. The correction is less for higher dielectric constants, since more of the fringing field is kept inside the cavity.

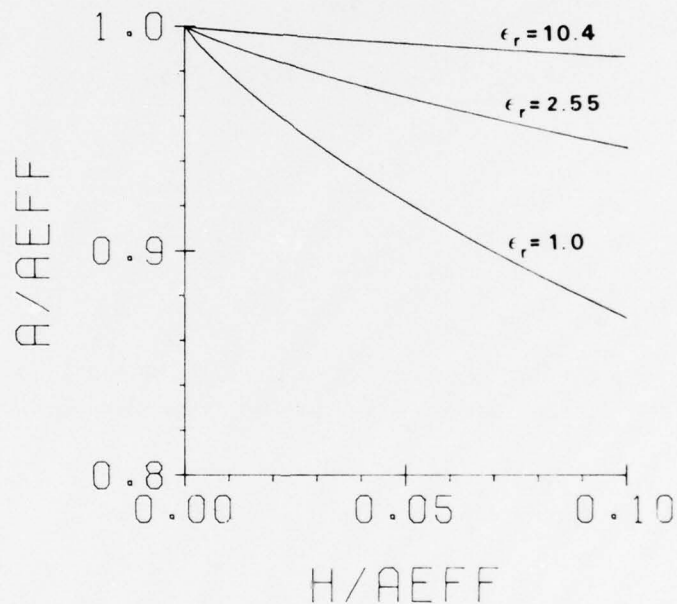


Figure 2. Correction of Disk Radius Due to Stray Fields

11. Shen, L.C., et al (1977) Resonant frequency of a circular disc, printed-circuit antenna, IEEE Trans. Antennas Propagation AP-25:595-596, July.

4. RADIATED POWER

The total radiated power is found by integrating the complex Poynting vector over a closed surface:

$$P_{\text{rad}} = \frac{1}{2} \operatorname{Re} \int \bar{\mathbf{E}} \times \bar{\mathbf{H}}^* \cdot d\bar{\mathbf{S}} \quad , \quad (6)$$

where $d\bar{\mathbf{S}}$ is the vector normal to the surface and the asterisk means complex conjugate. The power radiated through the upper half space is found by inserting the previously calculated far fields Eq. (3) into Eq. (6):

$$P_{\text{rad}} = \epsilon_{\text{no}} \cdot V_0^2 \cdot \frac{(k_0 \cdot a)^2}{960} \cdot \int_0^{\pi/2} \left[B_M^2(k_0 \cdot a \cdot \sin \theta) + \right. \\ \left. + \cos^2 \theta \cdot B_P^2(k_0 \cdot a \cdot \sin \theta) \right] \cdot \sin \theta \cdot d\theta \quad , \quad (7)$$

where

$$\epsilon_{\text{no}} = \begin{cases} 2 & n = 0 \\ 1 & n \neq 0 \end{cases} \quad .$$

A radiation conductance across the gap at $\psi = 0$ can be defined as a conductance that will dissipate the same power as that radiated by the circular disk:

$$G_{\text{rad}} = \epsilon_{\text{no}} \cdot \frac{(k_0 \cdot a)^2}{480} \cdot \int_0^{\pi/2} \left[B_M^2(k_0 \cdot a \cdot \sin \theta) + \right. \\ \left. + \cos^2 \theta \cdot B_P^2(k_0 \cdot a \cdot \sin \theta) \right] \cdot \sin \theta \cdot d\theta \quad . \quad (8)$$

The integral has been solved numerically and the radiation conductance for different modes is plotted in Figure 3 versus the disk-radius in free-space wavelength. As long as the antenna remains electrically thin, the radiation conductance is independent of the spacing between the disk and the groundplane.

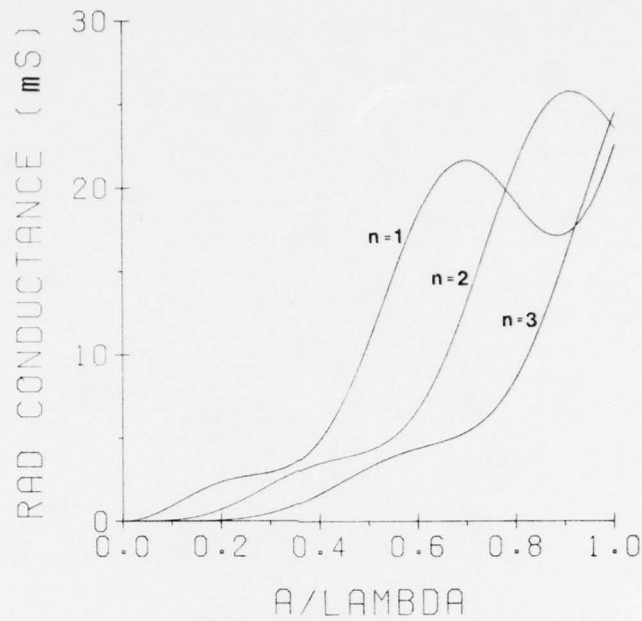


Figure 3. Radiation Conductance at Resonance of a Disk Antenna Excited in the TM Modes

5. DIRECTIVITY

The directivity of an antenna is defined as the ratio of the maximum power density to the average radiated power density. From the previously calculated far fields Eq. (3) and the total radiated power Eq. (7), the directivity of the circular disk excited in the $n = 1$ modes can be expressed as

$$D = \frac{(k_0 \cdot a)^2}{120 \cdot G_{\text{rad}}} \quad (9)$$

where G_{rad} is the radiation conductance as defined in Eq. (8). A plot of the directivity is shown in Figure 4 as a function of the free-space radius. It is independent of the thickness as long as the restrictions mentioned earlier are fulfilled. As the radius decreases, the directivity approaches 3, which is equivalent to 4.8 dB, as expected for a small slot in a groundplane. The directivity for an air-filled disk antenna is 9.9 dB, when excited in the dominant mode corresponding to a radius of 0.293 wavelength.

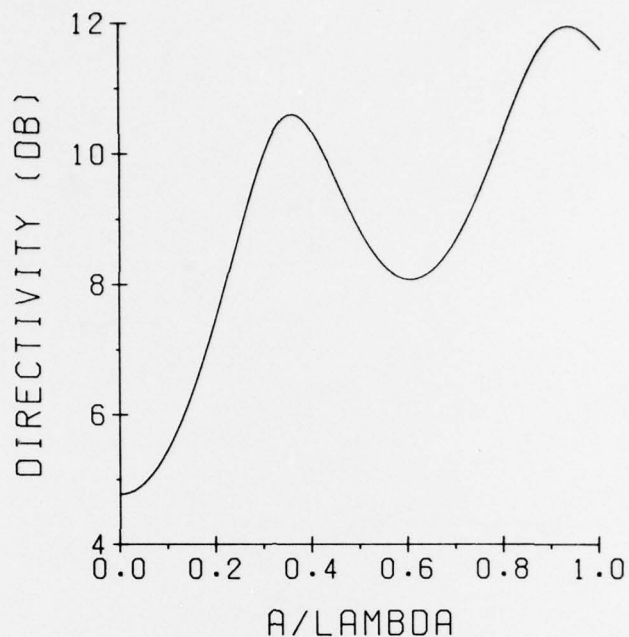


Figure 4. Directivity at Resonance of a Disk Antenna Excited in the TM_{1m} Modes

6. DIELECTRIC LOSSES

The power losses in the dielectric due to imperfect substrate can be obtained by means of a perturbation technique. The method is based on the assumption that introduction of small losses do not substantially change the fields from their loss-free values. The known loss-free field distribution is then used to evaluate the losses in the system, and from those an equivalent conductance can be determined. The losses are found by integrating the E-fields over the volume of the cavity:

$$P_{\text{diel}} = \frac{\omega \cdot \epsilon''}{2} \int \bar{E} \cdot \bar{E}^* dV \quad (10)$$

The dielectric substrate is characterized by the permittivity $\epsilon = \epsilon' - j\epsilon''$ and the loss tangent, $\tan \delta = \epsilon''/\epsilon'$. The circular disk antenna can be treated as a cavity, assuming the fields are contained between the disk and the groundplane. An equivalent conductance across the gap at $\psi = 0$ can be defined and calculated from Eqs. (1) and (10):

$$G_{\text{diel}} = \frac{\epsilon_{\text{no}} \cdot \tan \delta}{4 \cdot \mu_0 \cdot h \cdot f} [(k \cdot a)^2 - n^2] \quad (11)$$

The dielectric losses are proportional to the loss tangent of the dielectric as expected. The equivalent conductance is plotted in Figure 5 for a loss tangent of 0.0018, which has been assumed to be constant over the frequency band. For a given mode number, the dielectric losses decrease with increasing frequency and thickness. However, as the frequency is changed the physical radius of the disk must also be changed in order to fulfill the resonance conditions.

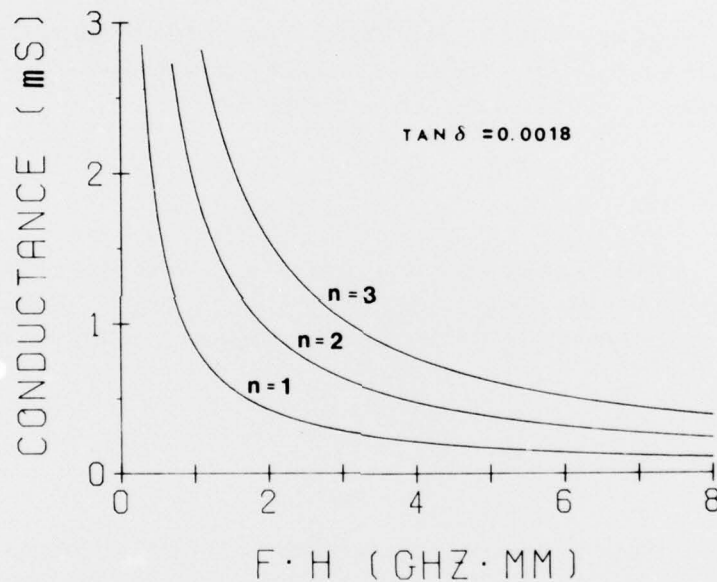


Figure 5. Equivalent Dielectric Conductance at Resonance of a Disk Antenna Excited in the TM_{n1} Modes

7. OHMIC LOSSES

The conductors always have a finite conductivity σ and, therefore, exhibit a surface impedance $R_S = 1/\sigma \cdot \delta_S$, where $\delta_S = (2/\omega\mu\sigma)^{1/2}$ is the skin depth. Generally it is very difficult to find the exact solutions of the fields when the conductors

have finite conductivity. However, if R_S is very small, the fields are very nearly that of the loss-free case. The power losses in the surface impedance is

$$P_{cu} = \frac{R_S}{2} \int \bar{K} \cdot \bar{K}^* dS, \quad (12)$$

where the integration is taken over the currents in the conductors. In our case the currents are derived from Eq. (1), assuming there are no fringing fields. An equivalent conductance across the gap at $\psi = 0$, which dissipates the same power as the conductors, can be determined by:

$$G_{cu} = \frac{\epsilon_{no} \cdot \pi(\pi \cdot f \cdot \mu_o)^{-3/2}}{4 \cdot h^2 \cdot \sqrt{\sigma}} [(k \cdot a)^2 - n^2]. \quad (13)$$

The equivalent conductance is plotted in Figure 6 for an effective conductivity of $1.0 \cdot 10^7$ S/m (reference 12). The ohmic losses become smaller as the frequency and the thickness are increased for a fixed-mode structure.

8. INPUT IMPEDANCE

The input impedance of the microstrip antenna at resonance is real. The fields between the disk and the groundplane are given by Eq. (1). If the feedpoint is located along the radius at $\psi = 0$, the input impedance can be expressed as

$$Z_{in}(\rho) = \frac{1}{G} \cdot \frac{J_n^2(k \cdot \rho)}{J_n^2(k \cdot a)}. \quad (14)$$

The total conductance G referred to the edge is the sum of the equivalent conductances due to radiation, dielectric, and ohmic losses given in Figures 3, 5, and 6, respectively. The normalized input impedance at resonance is plotted in Figure 7 for different mode numbers.

The total input conductance at resonance referred to the edge at $\psi = 0$ is given by Eqs. (8), (11), and (13). It has been plotted in Figures 8 and 9 for a disk excited in the dominant and the second mode. The dielectric constant is 2.55, the loss

-
12. Walton, M.D., et al (1977) An Experimental Measurement of the Radiation Fields and the Q-factor of a Circular Disc Antenna, Technical Report TR-77-02, Electromagnetics Laboratory, Dept. of Electrical Engineering, Univ. of Houston, Houston, TX.

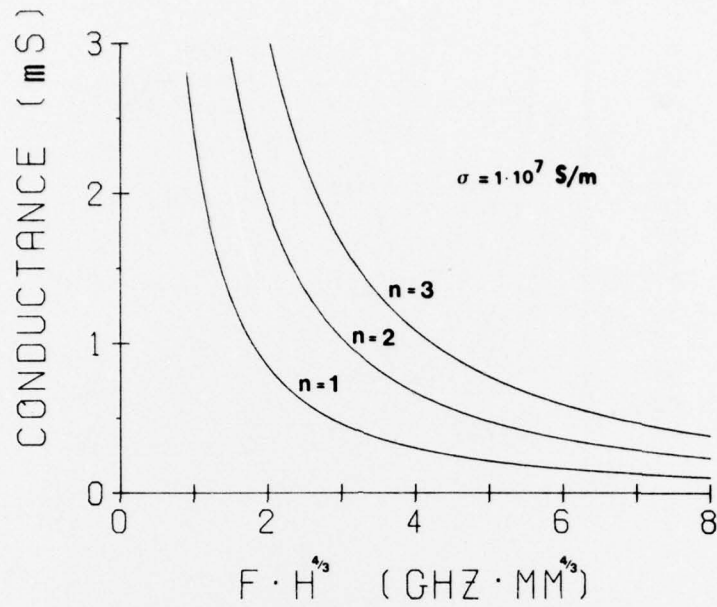


Figure 6. Equivalent Ohmic Conductance at Resonance of a Disk Antenna Excited in the TM_{n1} Modes

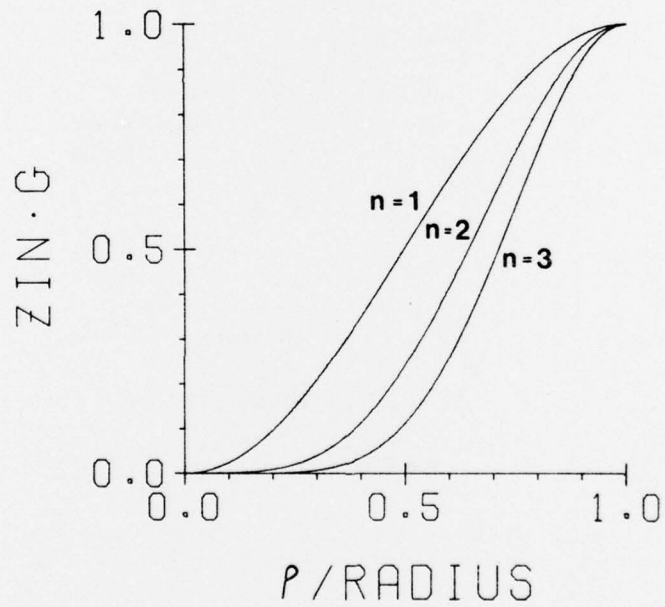


Figure 7. Normalized Input Impedance at Resonance of a Disk Antenna Excited in the TM_{n1} Modes as a Function of the Feed Point

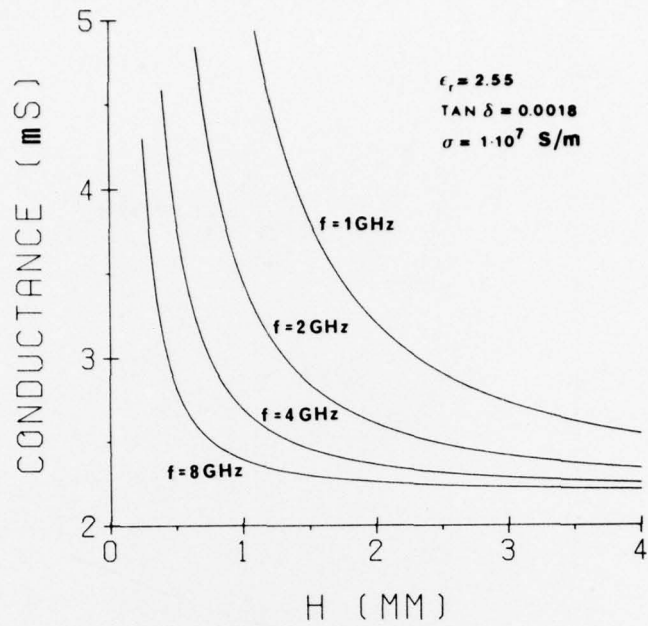


Figure 8. Total Input Conductance at Resonance of a Disk Antenna Excited in the TM_{11} Mode

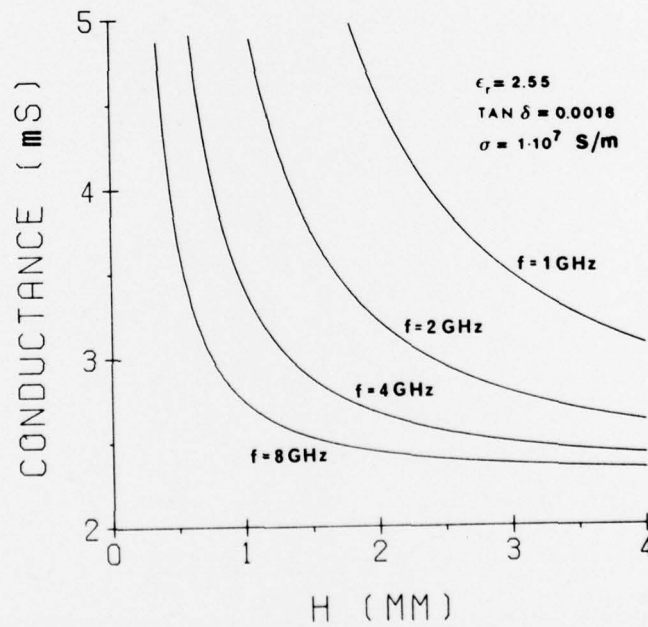


Figure 9. Total Input Conductance at Resonance of a Disk Antenna Excited in the TM_{21} Mode

tangent is 0.0018, and the conductivity is $1.0 \cdot 10^7$ S/m. The input conductance approaches the loss-free case as the frequency and the spacing are increased.

9. EFFICIENCY

The radiation efficiency of the microstrip disk as an antenna element is immediately found as the ratio between the radiated and the input powers. At resonance the efficiency is

$$\eta = \frac{G_{\text{rad}}}{G_{\text{rad}} + G_{\text{diel}} + G_{\text{cu}}} \quad (15)$$

where the equivalent conductances are given by Eqs. (8), (11), and (13). The radiation efficiency versus the spacing between the disk and the groundplane is shown in Figures 10 to 13. The dielectric constant chosen was 2.55, the loss tangent 0.0018, and the conductivity $1.0 \cdot 10^7$ S/m. The disk is resonant in the dominant mode in Figures 10 and 11, while it is excited in the second mode in Figures 12 and 13. The radiation efficiency increases with frequency and thickness, as long as the spacing is a small fraction of a wavelength. The air-filled cavity has a higher efficiency compared to the dielectric-filled one, in spite of a larger radius. All calculations are based on the loss-free field distributions, which means the results become less accurate as the radiation efficiency decreases.

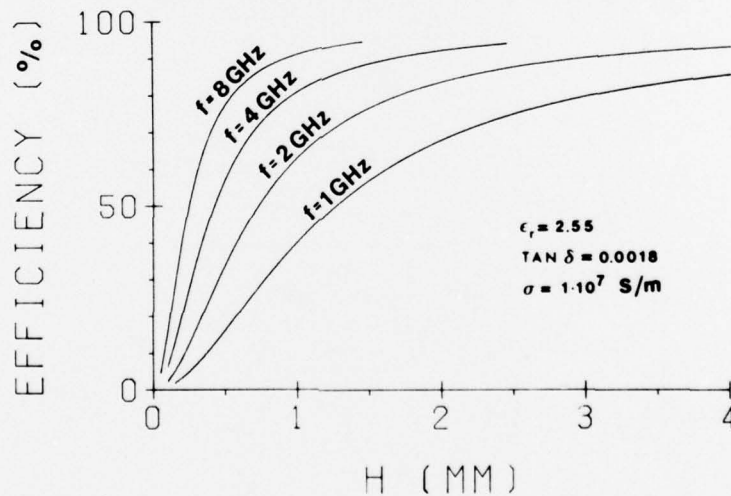


Figure 10. Radiation Efficiency at Resonance of a Disk Antenna Excited in the TM_{11} Mode

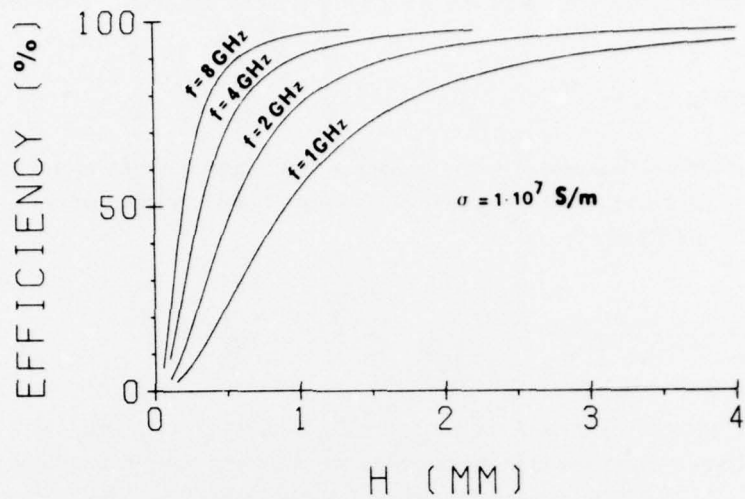


Figure 11. Radiation Efficiency at Resonance of an Air-Filled Disk Antenna Excited in the TM_{11} Mode

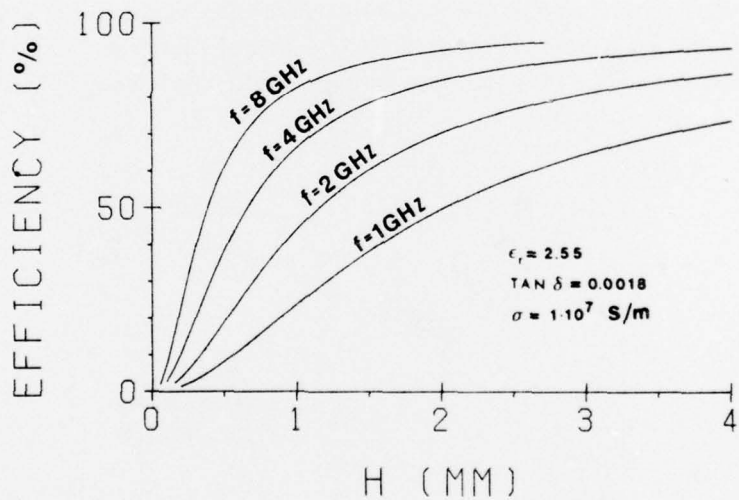


Figure 12. Radiation Efficiency at Resonance of a Disk Antenna Excited in the TM_{21} Mode

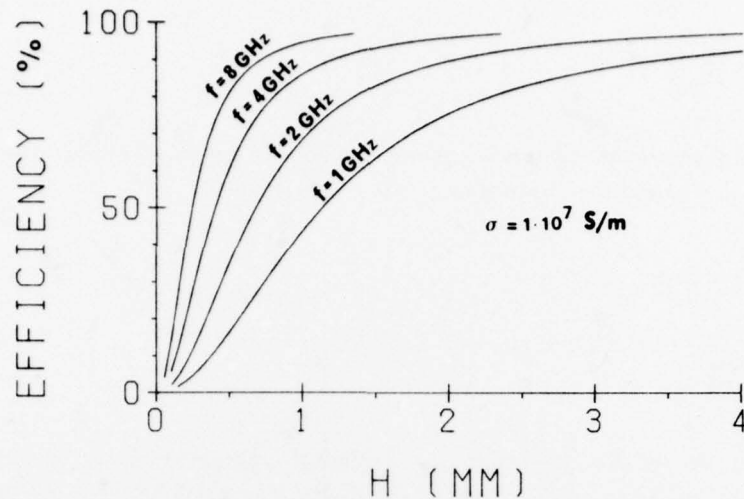


Figure 13. Radiation Efficiency at Resonance of an Air-Filled Disk Antenna Excited in the TM_{21} Mode

10. QUALITY FACTOR

A parameter specifying the frequency selectivity of a resonant circuit is the Q-factor. It is defined as the ratio between the energy stored in the system and the energy lost. At resonance the energy stored can be calculated from either the maximum magnetic fields or the maximum electric fields. In the latter case it is expressed as

$$W = \frac{\epsilon'}{2} \int \bar{E} \cdot \bar{E}^* dV \quad (16)$$

where the integration is taken over fields inside the cavity. In our case, the total energy stored is found from Eqs. (1) and (16):

$$W = \frac{\epsilon_{no} \cdot V_o^2}{16 \cdot \pi \cdot \mu_o \cdot h \cdot f^2} [(k \cdot a)^2 - n^2] \quad (17)$$

The Q-factor due to the radiation losses is determined by inserting Eqs. (7) and (17) into

$$Q_{\text{rad}} = \frac{\omega \cdot W}{P_{\text{rad}}} \quad (18)$$

In a similar way the Q-factors due to the losses in the dielectric and in the conductors are calculated from Eqs. (10), (12), and (16):

$$Q_{\text{diel}} = \frac{1}{\tan \delta} \quad (19)$$

$$Q_{\text{cu}} = \frac{h}{\delta_s} \quad (20)$$

The Q-factor due to the dielectric losses depends only on the loss tangent of the substrate and not on the dimensions of the disk. The ratio between the spacing of the disk and the groundplane and the skin depth determines the Q-factor caused by finite conductivity. The overall Q-factor can also be evaluated, which includes all of the losses:

$$\frac{1}{Q} = \frac{1}{Q_{\text{rad}}} + \frac{1}{Q_{\text{diel}}} + \frac{1}{Q_{\text{cu}}} \quad (21)$$

The total Q-factor has been plotted in Figures 14 and 15 for a circular disk excited in the dominant mode. The dielectric constant is 2.55, the loss tangent is 0.0018, and the conductivity is $1.0 \cdot 10^7$ S/m. The Q-factor decreases for larger spacings and higher frequencies, where the radiation losses are dominant. At small spacings, conductor losses prevail, giving a decreasing Q-factor. The air-filled cavity has a slightly lower Q than the dielectric-filled one, giving a broader bandwidth.

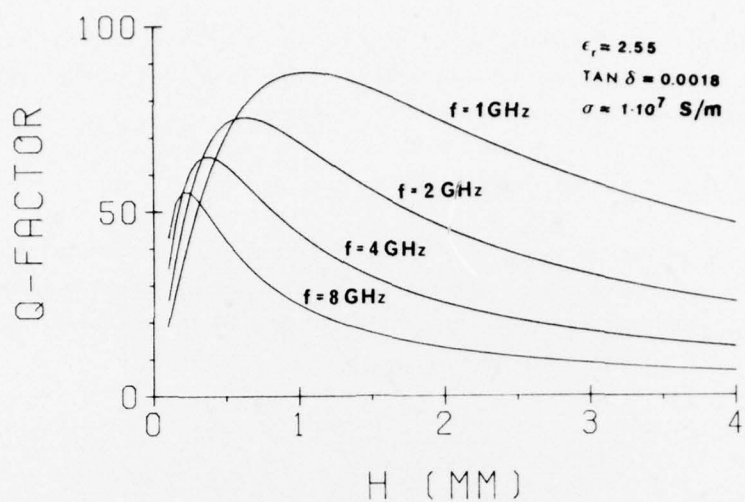


Figure 14. Quality Factor at Resonance of a Disk Antenna Excited in the TM_{11} Mode

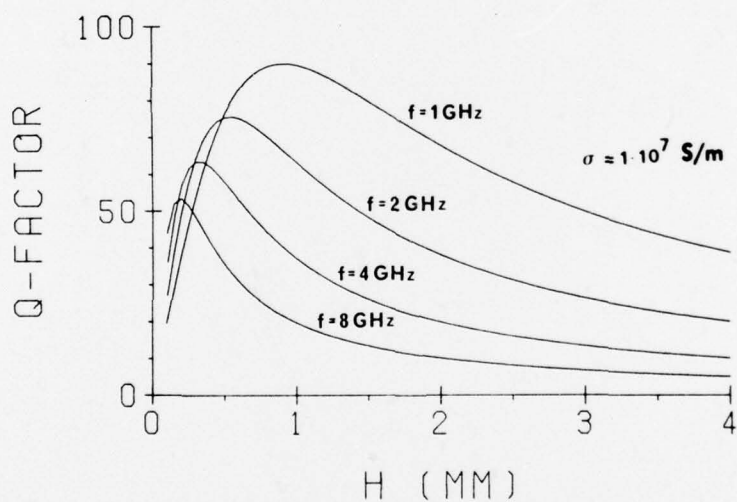


Figure 15. Quality Factor at Resonance of an Air-Filled Disk Antenna Excited in the TM_{11} Mode

11. CIRCULAR POLARIZATION

Circularly polarized radiated fields may be constructed by exciting two orthogonal modes on the disk with 90 degrees phase difference. The E-field across the aperture then becomes

$$E_Z = E_0 \cdot J_n(k \cdot a) \cdot (\cos n\psi \pm j \cdot \sin n\psi) \quad , \quad (22)$$

where the plus sign refers to left-hand circular polarization and minus sign to right-hand circular polarization. The far-fields are calculated in a way similar to the previous ones. In general, the radiated fields will be elliptically polarized with an axial ratio expressed in decibels as

$$AR = 20 \cdot \left| \log \frac{B_P(k_0 \cdot a \cdot \sin \theta) \cdot \cos \theta}{B_M(k_0 \cdot a \cdot \sin \theta)} \right| \quad . \quad (23)$$

This is a function of the polar angle and the radius of the disk, but it is independent of ψ because of the cylindrical symmetry of the disk. The axial ratio of a circularly polarized disk antenna excited in the dominant mode is plotted in Figure 16

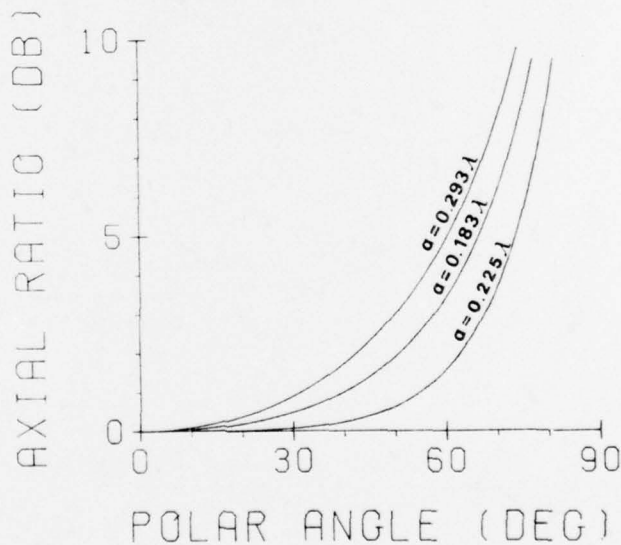


Figure 16. Axial Ratio of a Circularly Polarized Disk Antenna Excited in the TM_{11} Mode

versus the polar angle. A general requirement is to obtain low axial ratios for all directions within a specified angle from the beam center. The parameter to choose is the dielectric constant of the substrate, giving different resonance radii of the disk.

12. SUMMARY AND DISCUSSION

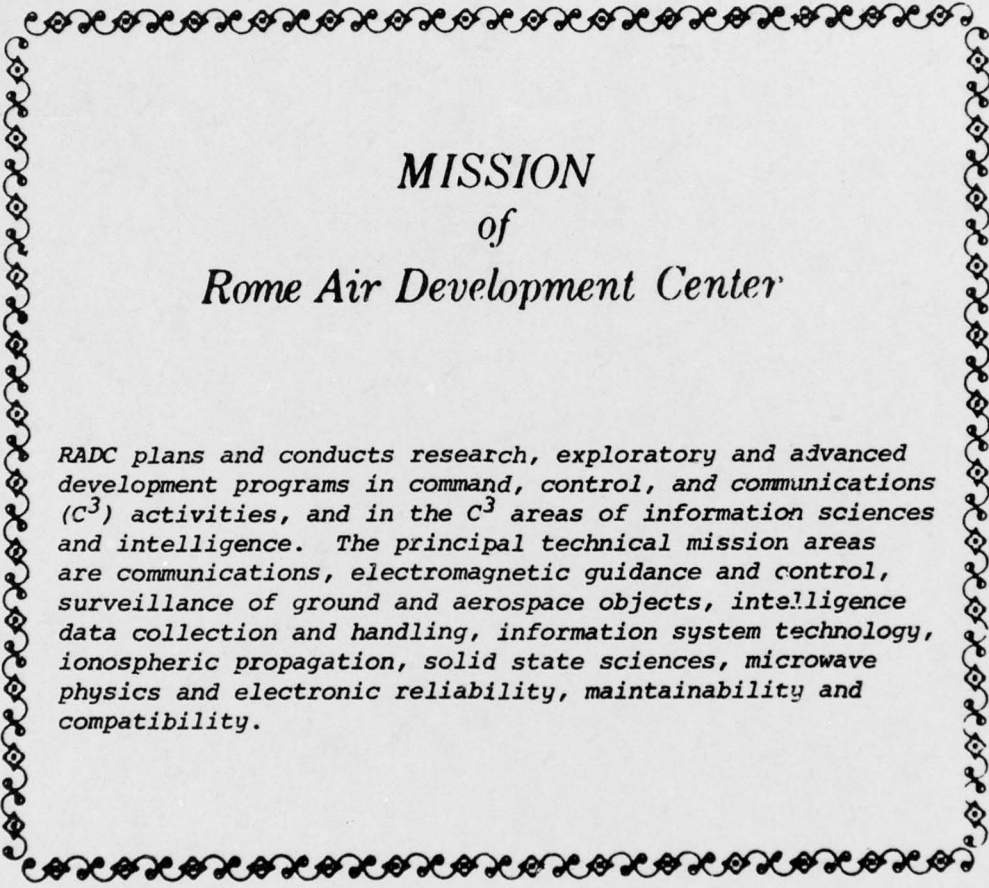
The properties of the microstrip disk antenna element, with or without a supporting dielectric sheet, have been expressed in graphs and formulas for design purposes. The theory is restricted to small spacings between the disk and the groundplane compared to the wavelength and the radius of the disk. The antenna element is modeled as a cylindrical cavity with a magnetic wall along the side. This simplification takes neither the size of the groundplane nor the stray fields into account. However, the fringing fields are considered when the resonance conditions are determined, giving values of the radius very close to experimental data. The TM_{11} mode has the lowest resonance frequency and it is, therefore, the dominant one. The $n = 1$ modes are the only ones that radiate normal to the disk.

The loss calculations and, therefore, also the efficiency and the Q-factor results are based on the field distributions of the loss-free case. Practical microwave antennas are designed with low losses not limiting the validity of the results. A higher efficiency and a broader bandwidth at a fixed frequency are achieved with a low dielectric constant and a large thickness.

The input impedance at resonance is made up of equivalent conductances due to radiation, dielectric, and ohmic losses. Calculations show that the element can be matched to all practical impedance levels by varying the feed point along the radius of the disk.

References

1. Howell, J.Q. (1975) Microstrip antennas, IEEE Trans. Antennas Propagation, AP-23:90-93.
2. Parks, F.G., and Bailey, M.C. (1977) A low sidelobe microstrip array, IEEE AP-S Intl. Symp. Digest, pp. 77-80, June.
3. Stockton, R.J., and Hockensmith, R.P. (1977) Application of spherical arrays - a simple approach, IEEE AP-S Intl. Symp. Digest, pp. 202-205, June.
4. Agrawal, P.K., and Bailey, M.C. (1976) An analysis technique for microstrip antennas, IEEE AP-S Intl. Symp. Digest, pp. 395-398, Oct.
5. Coffey, E.L. (1977) Microstrip antenna far-field radiation pattern analysis using the unimoment-Monte Carlo method, IEEE AP-S Intl. Symp. Digest, pp. 276-279, June.
6. Long, S.A., and Shen, L.C. (1977) The circular disc, printed circuit antenna, IEEE AP-S Intl. Symp. Digest, pp. 100-103, June.
7. Long, S.A., et al (1977) The Theory of the Circular Disc, Printed Circuit Antenna, Technical Report TR-77-01, Electromagnetics Laboratory, Dept. of Electrical Engineering, Univ. of Houston, Houston, TX.
8. Watkins, J. (1969) Circular resonant structures in microstrip, Electron. Lett. 5:524-525, Oct.
9. Kernweis, N.P., and McIlvanna, J.F. (1977) Liquid crystal diagnostic techniques an antenna design aid, Microwave Journal 20:47-51, 58, Oct.
10. Martin, E.J. Radiation fields of circular loop antennas by a direct integration process, IRE Trans. Antennas Propagation, AP-8:105-107, Jan.
11. Shen, L.C., et al (1977) Resonant frequency of a circular disc, printed-circuit antenna, IEEE Trans. Antennas Propagation AP-25:595-596, July.
12. Walton, M.D., et al (1977) An Experimental Measurement of the Radiation Fields and the Q-factor of a Circular Disc Antenna, Technical Report TR-77-02, Electromagnetics Laboratory, Dept. of Electrical Engineering, Univ. of Houston, Houston, TX.



*MISSION
of
Rome Air Development Center*

RADC plans and conducts research, exploratory and advanced development programs in command, control, and communications (C³) activities, and in the C³ areas of information sciences and intelligence. The principal technical mission areas are communications, electromagnetic guidance and control, surveillance of ground and aerospace objects, intelligence data collection and handling, information system technology, ionospheric propagation, solid state sciences, microwave physics and electronic reliability, maintainability and compatibility.

78